# RSC Applied Polymers



**PAPER** 

View Article Online
View Journal | View Issue



**Cite this:** *RSC Appl. Polym.*, 2025, **3**, 897

# Flexible self-healing polyborosiloxane-based triboelectric nanogenerators for environmental adaptability

Jiahui Liang,<sup>a</sup> Run Zhao,<sup>b</sup> Jiale Li,<sup>b</sup> Ding Zhao,<sup>b</sup> Panlei Liu,<sup>a</sup> Changyong Tian\*<sup>c</sup> and Na Sun <sup>b</sup> \*

The rapid increase in energy consumption has heightened interest in harnessing energy from natural mechanical motion. Triboelectric Nanogenerators (TENGs), based on triboelectric and electrostatic induction, offer a promising solution due to their simple structure, low cost, and high energy conversion efficiency under low-frequency motion. This study presents the development of flexible, self-healing triboelectric materials based on viscoelastic polyborosiloxanes (PBS), designed to enhance the performance and environmental adaptability of TENGs. The PBS films exhibit excellent shape adaptability and adhesiveness, enabling them to adhere to irregular surfaces and achieve a self-healing efficiency of 93.2% within 3 minutes at room temperature. The incorporation of boric acid as a cross-linking agent significantly improves the electrical output performance, with the open-circuit voltage  $(V_{OC})$  and short-circuit charge (Q<sub>sc</sub>) increasing by 15% and 20%, respectively, at a boric acid content of 33 wt%. Despite the decrease in tensile strength with higher boric acid content, the PBS-based TENGs maintain stable electrical output under varying load conditions and demonstrate superior performance at low frequencies. The fabricated TENG devices, utilizing PBS and copper films as triboelectric materials, effectively convert a pulsed alternating current into direct current, providing a stable power supply for small electronic devices. These findings underscore the potential of PBS-based flexible, self-healing triboelectric materials for energy harvesting and portable electronic applications, particularly in environments with irregular mechanical sources.

Received 7th January 2025, Accepted 13th April 2025 DOI: 10.1039/d5lp00006h

rsc.li/rscapplpolym

### Introduction

With the rapid increase in energy consumption, there has been growing attention on harnessing energy from natural mechanical motion. Triboelectric Nanogenerators (TENGs) based on triboelectric and electrostatic induction, and to their simple structure, low cost, and high energy conversion efficiency under low-frequency motion, enable the utilization of various forms of mechanical energy such as wind, human motion, structural vibrations, and ocean waves. However, the mechanical sources in natural environments are mostly irregular low-frequency motions, and TENGs, due to their inherent internal capacitance, typically output a high voltage but low current. Consequently, under insufficient input conditions, the performance of TENGs significantly declines, limiting their application in power supply,

sensing, and other portable devices.<sup>6</sup> To achieve further commercialization of TENGs, it is critical to maintain excellent performance output under complex mechanical source inputs.

In recent years, researchers have attempted various methods to adapt to complex mechanical source inputs, but the adaptability of triboelectric materials to complex mechanical sources has not been deeply studied. Kim et al.7 used gear and crankslider mechanisms to increase the operating frequency of TENGs, enhancing their output, but with low space utilization, and only investigated the effect of frequency on output. Cheng et al.8 adopted a triangular cam mechanism for stable output, vet the constant-speed motion of the follower induces significant inertial effects on the TENG. Han et al.9 combined energy storage structures, escapement mechanisms, and resonators to continuously collect low-frequency mechanical energy from the environment, but their complex structural design and rotating triboelectric mode result in severe material wear. Nuthalapati et al.10 reported a high-performance MWCNTs/PDMS nanocomposite-based TENG for haptic applications, achieving an open-circuit voltage of ~249 V, a short-circuit current of  $\sim$ 28.03  $\mu$ A, and a power density of 2.81 W m<sup>-2</sup>. This study high-

<sup>&</sup>lt;sup>a</sup>School of Mechanical Engineering, Beijing Institute of Technology, Beijing 100081, P.R. China. E-mail: nsun@bit.edu.cn

<sup>&</sup>lt;sup>b</sup>Beijing 101 Middle School, Beijing 100091, P.R. China

<sup>&</sup>lt;sup>c</sup>Technical Institute of Physics and Chemistry, Chinese Academy of Sciences, Beijing 100190, P.R. China. E-mail: tcy@mail.ipc.ac.cn

lights the potential of flexible and biocompatible materials, such as PDMS and MWCNTs, to improve the performance of TENGs for wearable and haptic applications. Hajra et al. 11 explored self-powered actuation systems based on TENGs, enhancing their efficiency and reliability. The study also included the development of TENG-based pressure sensors, integrated with robotic grippers for enhanced functionality. The selection of triboelectric materials is crucial during the triboelectric process, as traditional rigid material contacts are difficult to achieve completely and are prone to mechanical damage, such as scratching and collision during long-term practical applications, leading to a decline in the electrical performance of TENGs, or even failure. 12 Potu et al. 13 presented a cost-effective TENG design utilizing overhead projector (OHP) sheets and ZnO nanosheet array films. The study leveraged the excellent electron mobility and biocompatibility of oxide materials (OM), demonstrating their potential for diverse energy harvesting applications.14 Rani et al.15 introduced biocompatible TENG-based edible electronic skins made from chitosan films, which exhibited promising performance in selfpowered applications. The electrical output of these e-skins was validated by charging commercial capacitors and powering low-energy electronic devices, such as LEDs. Sun et al. 16 introduced dynamic imine bonds into PDMS to prepare flexible selfhealing triboelectric layers, but required 12 hours to achieve self-healing after damage. Deng et al.17 used a glassy elastomer based on dynamic disulfide bonds as a triboelectric layer, requiring 4 hours to achieve self-healing at 65 °C.

In this study flexible self-healing triboelectric materials were prepared with good environmental adaptability based on viscoelastic polyborosiloxanes (PBS), avoiding the introduction of mechanical structures and reducing the conversion efficiency of mechanical energy in the environment through good adaptability of triboelectric materials to irregular mechanical sources. Crosslinked with terminal hydroxyl polydimethylsiloxane and HB, dynamic hydrogen bonds and coordination bonds are formed between boron and oxygen molecules, giving PBS room-temperature self-healing properties. The influence of HB on the electrical output performance and mechanical properties of PBS was investigated. As the HB content increased, the tensile strength of PBS gradually decreased, while the electrical performance output showed an upward trend. When the ratio of PDMS-OH to HB was 3:1, the open-circuit voltage  $(V_{oc})$  and short-circuit charge  $(Q_{sc})$ were 164 V and 53 nC, respectively. A self-healing efficiency of 93.2% was achieved in air within 3 minutes. In studies involving varying frequencies, loading modes, and loading durations, PBS maintained an output of over 120 V. Using PBS  $(25 \times 25 \text{ mm}^2)$  as the triboelectric material, the fabricated TENG devices could illuminate 43 commercial LED lights with a simple finger press.

# **Experimental section**

#### Preparation of PBS films

Hydroxyl-terminated polydimethylsiloxane  $(OH-(C_2H_6OSi)_n-H, PDMS-OH)$  was purchased from Alfaesa (China) Chemical Co.,

Ltd. Anhydrous ethanol (analytical grade) was obtained from Beijing Chemical Plant. Boric acid (BA, purity 99%) was sourced from Tianjin Yongda Chemical Reagent Co., Ltd. The composite films were prepared using a solution blending method. Initially, varying masses of boric acid (0.5 g, 1 g, 2 g, and 3 g) were dissolved in 30 mL of anhydrous ethanol and fully dissolved by magnetic stirring for 15 minutes. Subsequently, 6 g of hydroxylterminated polydimethylsiloxane (PDMS-OH) was added, and the solution was placed in an oil bath with a stirrer, reacting at 190 °C for 1 hour until the ethanol was fully evaporated. Postreaction, the PBS was allowed to cool for 24 hours and then compression molded into 1 mm thick PBS films and cut into 25 mm × 25 mm samples for testing. Fig. 1(a) shows the schematic diagram of the PBS film preparation process.

#### Characterization of PBS films

The molecular structure of the PBS films was analyzed and identified using a Bruker Tensor 27 Fourier transform infrared spectrometer (FTIR, Bruker Optics Co. Ltd, Germany). The tensile strength of the films was characterized using a universal tensile tester (model HD-B609A-S, Haida International Instruments Co., Ltd, China). Following the GB/T528-2009 standard, the samples were fabricated into dumbbell shapes, and the tensile testing speed was set at 50 mm min<sup>-1</sup>. Three independent specimens of each sample type were prepared, and tensile tests were performed on each specimen under identical conditions.

#### Preparation of TENGs

The fabricated contact-separation triboelectric nanogenerator primarily consists of upper and lower substrates, upper and lower electrodes, and PBS films, as illustrated in Fig. 1(b). The upper and lower substrates are made of polymethyl methacrylate (PMMA), with copper foil serving as the electrode material. PBS acts as the negative triboelectric layer, forming a contact pair with the upper copper foil.

#### **Electrical performance of TENGs**

Fig. 1(c) and (d) show the contact-separation mode and the triboelectric performance test platform, which includes an electrometer (Keithley 6514), a pressure sensor, a stepper driver, a motor speed controller, and a DC power supply. During the experiment, the loading method and loading time were controlled by altering the shape of the cam, as shown in Fig. 1(e) and (f).

## Results and discussion

# Surface morphology and infrared spectral characteristics of PBS films

Fig. 2 illustrates the surface morphology of PBS films. As a viscoelastic polymer material, PBS exhibits a smooth and flat surface, as evidenced by the optical photograph in Fig. 2(a). Fig. 2(b) demonstrates that PBS possesses a certain degree of adhesiveness, allowing it to adhere to the body easily. This characteristic makes PBS an excellent, flexible material capable of adhering to irregular surfaces.

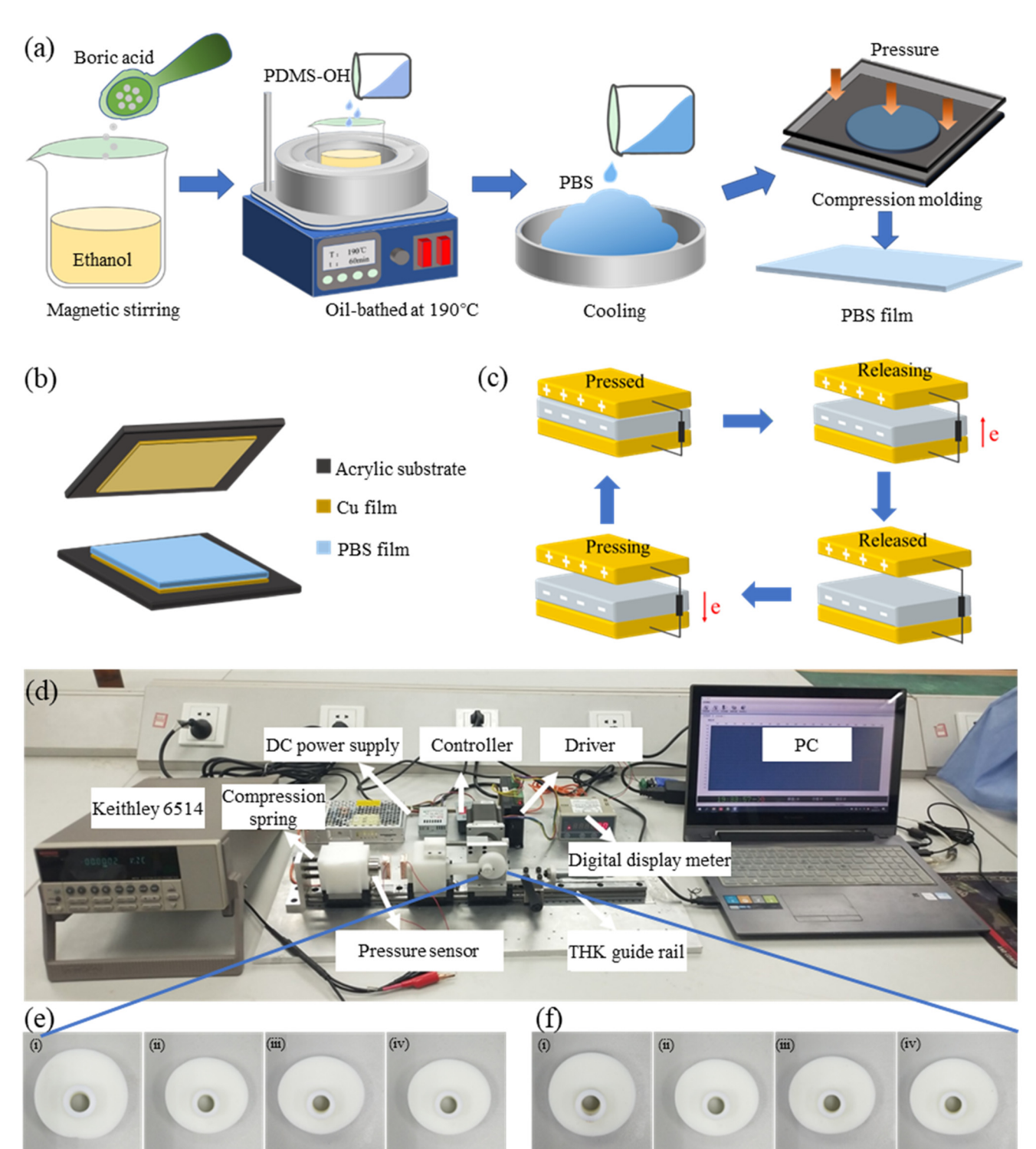


Fig. 1 (a) Schematic diagram of the PBS film preparation process; (b) schematic diagram of a TENG based on PBS films; (c) schematic showing the contact-separation mode; (d) contact-separation mode triboelectric performance test platform; (e) cams with different follower motion profiles: (i) constant velocity, (ii) constant acceleration, (iii) simple harmonic motion, and (iv) cycloidal motion; and (f) cams with different dwell angles: (i) 30°, (ii) 60°, (iii) 90°, and (iv) 120°.

Fig. 2(c) presents the infrared spectroscopy analysis of PBS (25 wt%). The spectrum reveals a stretching vibration peak at 2962 cm<sup>-1</sup> corresponding to the CH<sub>3</sub> groups on the siloxane. The peak at 1340 cm<sup>-1</sup> is attributed to the stretching vibration of Si-O-B, while the peak at 1007 cm<sup>-1</sup> corresponds to the main chain Si-O-Si stretching vibration.

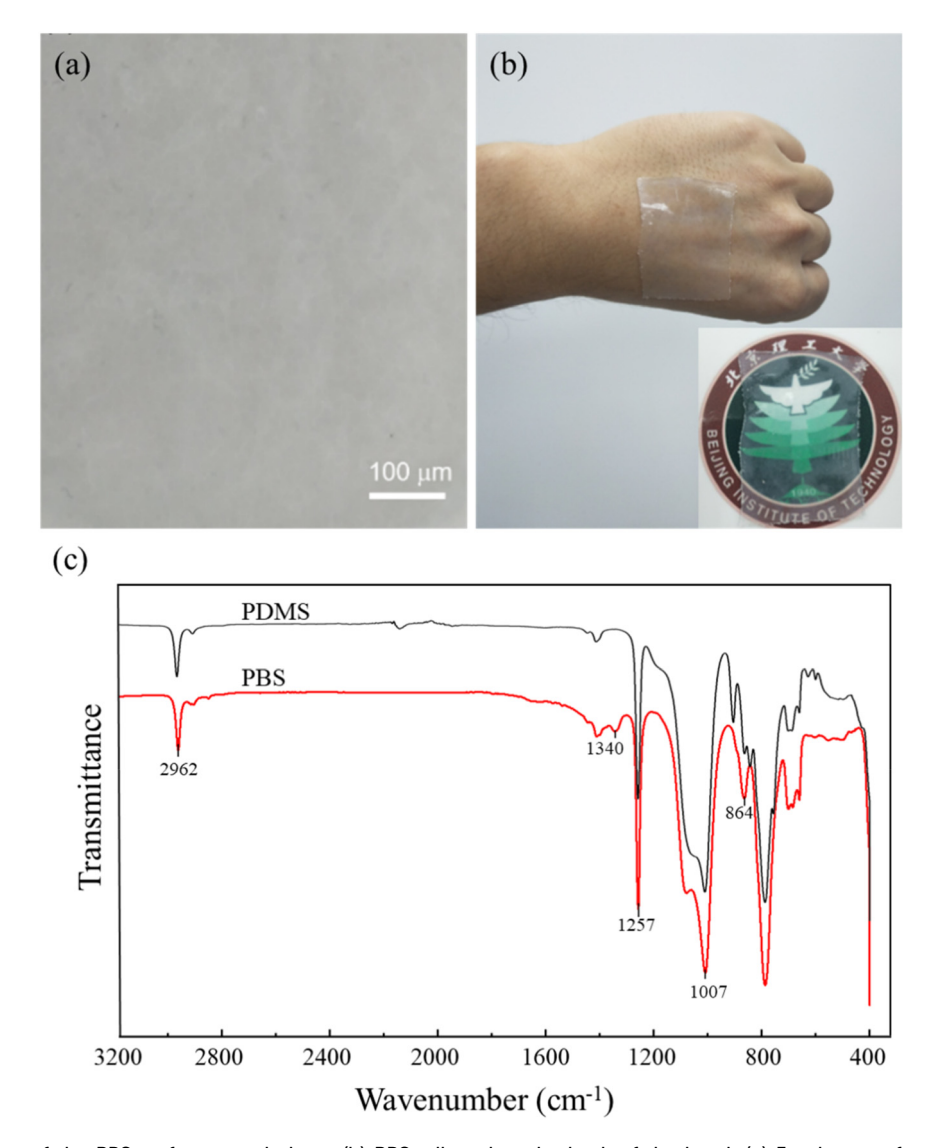


Fig. 2 (a) Optical image of the PBS surface morphology; (b) PBS adhered to the back of the hand; (c) Fourier transform infrared spectroscopy spectra of PBS.

Additionally, the peaks at 1257 cm<sup>-1</sup> and 864 cm<sup>-1</sup> are associated with the stretching vibrations of Si(CH<sub>3</sub>)<sub>2</sub>. The absorption peak at 1340 cm<sup>-1</sup> confirms the formation of Si-O-B within the molecular chain, indicating the incorporation of boron atoms into the siloxane main chain. This finding reinforces the hypothesis that B-O electron bridges play a crucial role in enhancing self-healing efficiency. Moreover, the presence of Si-O-Si and Si(CH<sub>3</sub>)<sub>2</sub> groups suggests the potential for hydrogen bonding interactions, consistent with observations in analogous polymer systems.18

#### Mechanical properties of PBS films

Fig. 3 presents the tensile strength measurements of PBS films with varying boric acid content. As the boric acid content increases, the tensile strength of PBS gradually decreases. When the boric acid mass fraction is 8 wt%, the stress of PBS

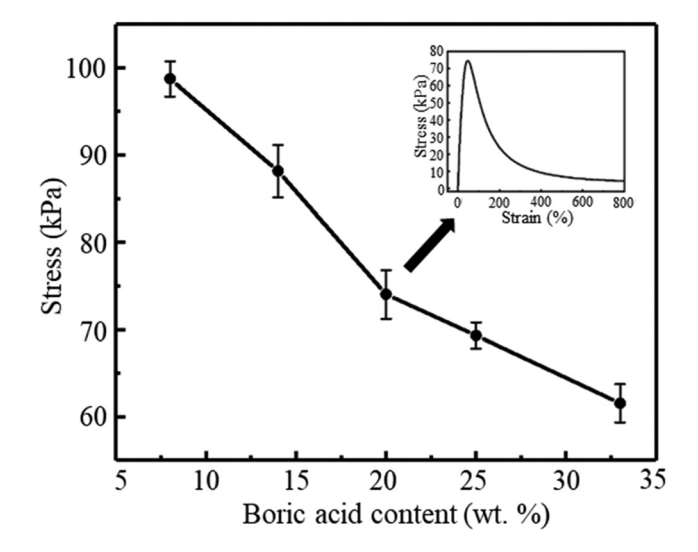


Fig. 3 Tensile strength of PBS films with different boric acid contents.

is 98.7 kPa. However, when the mass fraction increases to 33 wt%, the tensile strength decreases to 61.5 kPa, representing a 38% reduction. The primary reason for this trend is that at lower boric acid content, the resulting PBS exhibits a higher boron cross-linking density, leading to stronger intermolecular forces and consequently higher tensile strength. <sup>19</sup>

#### Self-healing properties of PBS films

Fig. 4 illustrates the self-healing process of PBS films. When PBS is severed, as shown in Fig. 4(b), it undergoes self-healing in air at room temperature (27  $\pm$  1  $^{\circ}$ C) for 3 minutes, as depicted in Fig. 4(c). PBS regains its original tensile properties upon stretching, as demonstrated in Fig. 4(d).

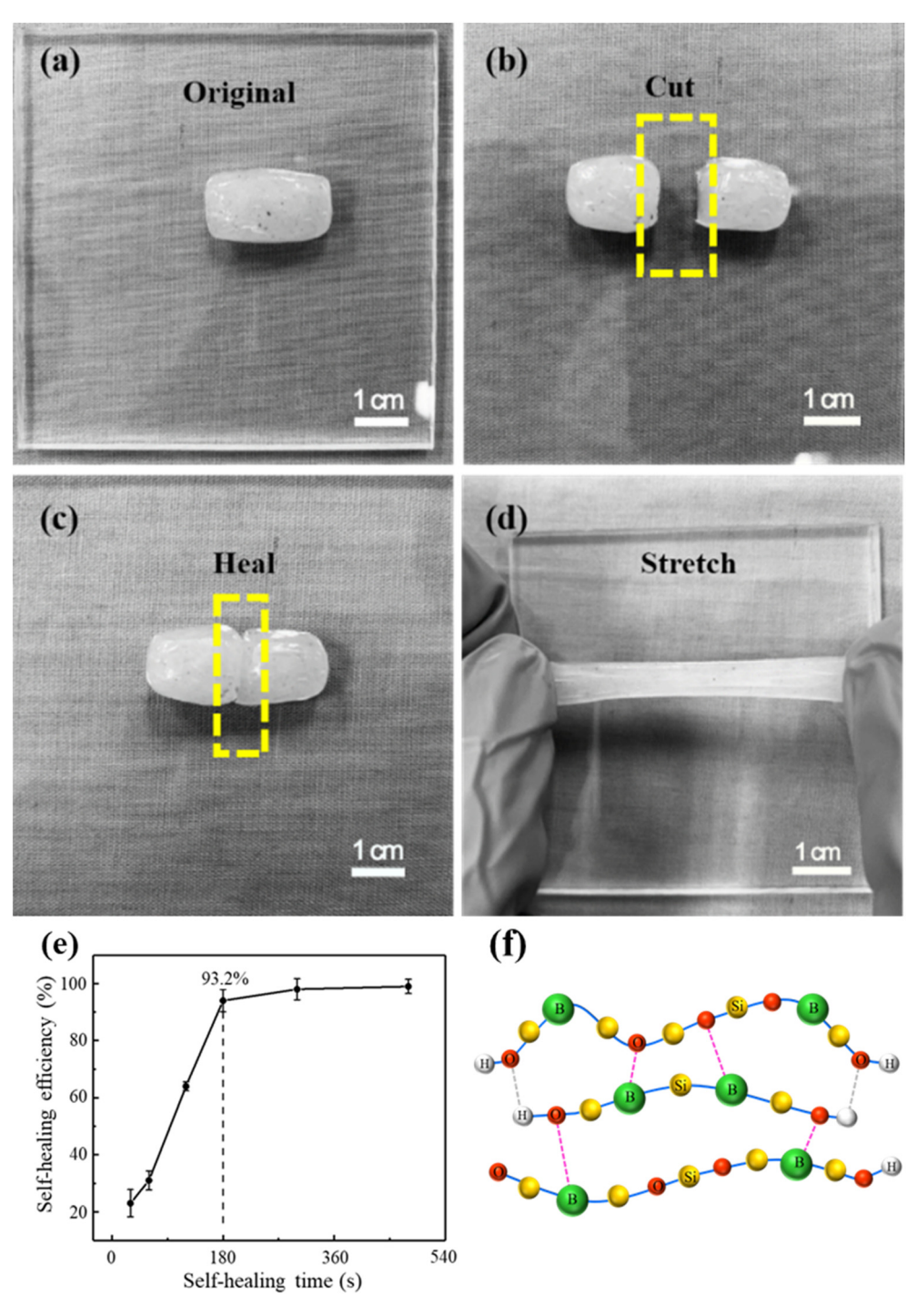


Fig. 4 Self-healing process of PBS: (a) initial state; (b) severed; (c) healed; (d) stretched; (e) relationship between self-healing efficiency and time; and (f) schematic diagram of the internal cross-linking structure of PBS.

**Paper** 

The self-healing efficiency of PBS is defined using tensile tests as

 $\eta = \delta_1/\delta_0$ 

where  $\delta_0$  and  $\delta_1$  represent the tensile strength of PBS before and after self-healing, respectively.

Fig. 4(e) shows the relationship between self-healing efficiency and time for PBS with 25 wt% boric acid content in air, indicating that a self-healing time of 3 minutes can achieve a self-healing efficiency of 93.2%. PBS is a key derivative of polydimethylsiloxane (PDMS). It represents a significant branch of polydimethylsiloxane (PDMS) derivatives, which is achieved by incorporating boron elements into the main chain. The self-healing mechanism of PBS is attributed to its internal cross-linking structure. As illustrated in Fig. 4(f), the boron atoms in the Si–O–B units of the polyborosiloxane molecular chain can form B–O electron bridges with oxygen atoms in adjacent chains. These electron bridges are dynamic physical cross-links, continuously dissociating and reforming. The self-healing are self-healing efficiency of 93.2%. PBS is a key derivative of 93.2%. PBS is a key deri

Unreacted –OH functional groups form dynamic hydrogen bonds.<sup>22</sup>

# Electrical performance of PBS-based triboelectric nanogenerators

Fig. 5(a) illustrates the impact of varying boric acid content on the electrical output performance. When the boric acid mass fraction is 8 wt%, the open-circuit voltage ( $V_{\rm oc}$ ) and short-circuit charge ( $Q_{\rm sc}$ ) are 146 V and 45 nC, respectively. As the boric acid content increases, both  $V_{\rm oc}$  and  $Q_{\rm sc}$  gradually rise. At a boric acid content of 33 wt%,  $V_{\rm oc}$  and  $Q_{\rm sc}$  reach 168 V and 55 nC, representing increases of 15% and 20%, respectively.

This enhancement arises from boric acid serving as a crosslinking agent for PDMS-OH while introducing unreacted H<sup>+</sup> ions as dopants. The mechanism lies in the electron-accepting capability of H<sup>+</sup> cations, which possess empty 1s orbitals that efficiently capture electrons. This interaction significantly enhances the material's electronic properties.<sup>23</sup> Moreover, the presence of H<sup>+</sup> cations within the polymer matrix facilitates charge transfer and retention, boosting triboelectric perform-

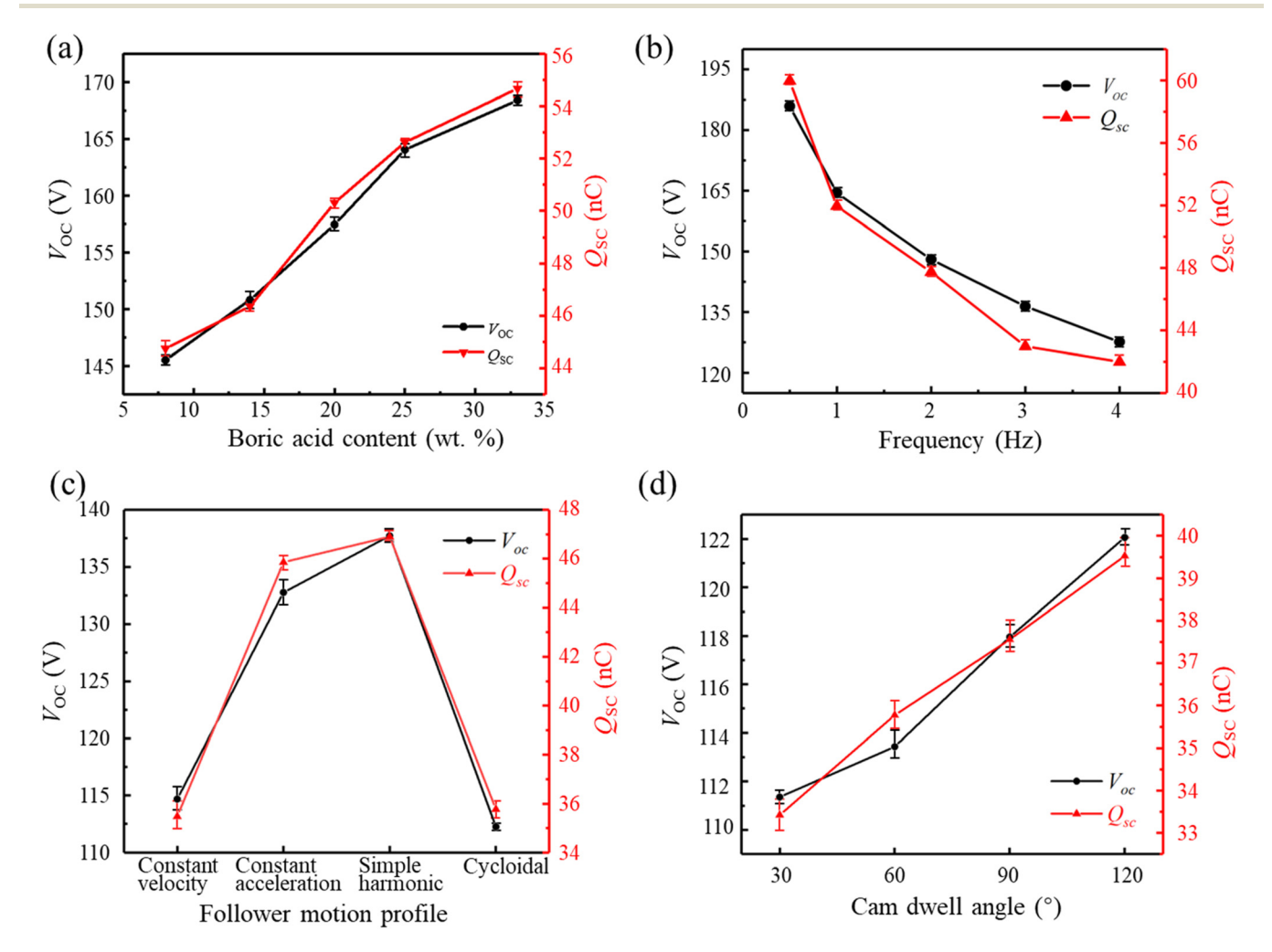


Fig. 5 Influence of different parameters on electrical output performance: (a) boric acid content; (b) frequency; (c) follower motion profile; and (d) cam dwell angle.

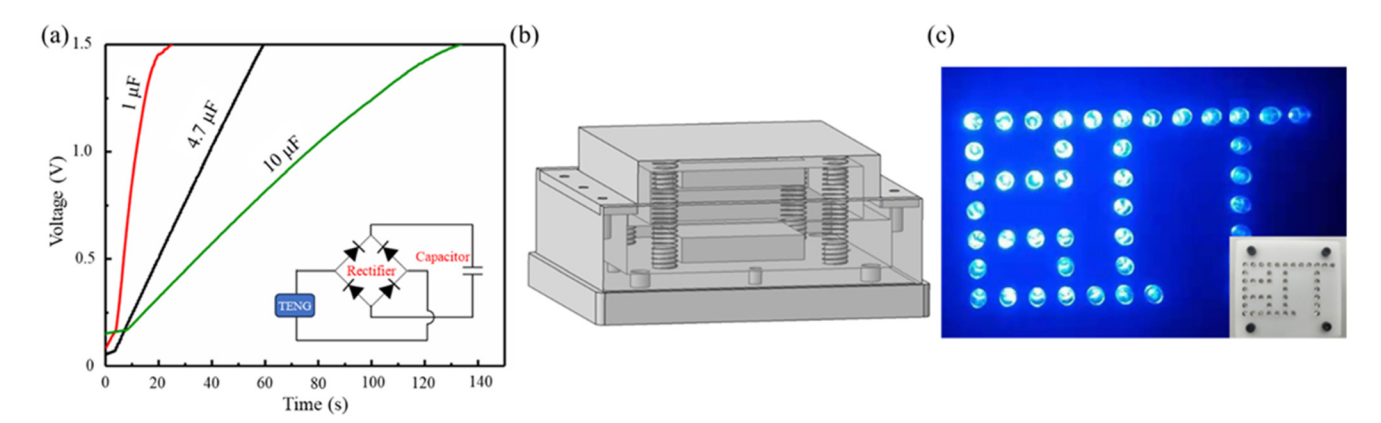


Fig. 6 (a) Charging curve of the capacitor by the TENG; (b) structural diagram of the TENG device; and (c) photograph of illuminated commercial LED lights.

ance. Additional references substantiate this explanation. Fig. 5(b) presents the electrical output performance at different testing frequencies (0.5–4 Hz). As the frequency increases, both  $V_{\rm oc}$  and  $Q_{\rm sc}$  exhibit a decreasing trend. At 0.5 Hz,  $V_{\rm oc}$  and  $Q_{\rm sc}$  are 185 V and 59 nC, respectively. When the frequency increases to 4 Hz,  $V_{\rm oc}$  and  $Q_{\rm sc}$  decrease to 127 V and 41 nC, representing reductions of 31% and 30%, respectively. This decline is due to the reduced contact pressure and time at higher frequencies, altering the contact state and thus decreasing output performance. PBS demonstrates superior output performance under low-frequency conditions.  $^{25}$ 

The loading mode and duration also affect the output performance of TENGs. Fig. 5(c) shows the impact of different loading modes on PBS output performance, with constant acceleration and cosine loading modes yielding higher outputs. Under cosine loading,  $V_{\rm oc}$  and  $Q_{\rm sc}$  are 137 V and 46 nC, respectively, while under sine loading, the outputs are lower at 112 V and 35 nC.

Fig. 5(d) illustrates the effect of loading duration on PBS output performance under cosine loading.  $V_{\rm oc}$  and  $Q_{\rm sc}$  increase with longer loading times. At a dwell angle of 30°,  $V_{\rm oc}$  and  $Q_{\rm sc}$  are 111 V and 33 nC, respectively. When the dwell angle increases to 120°,  $V_{\rm oc}$  and  $Q_{\rm sc}$  rise to 122 V and 39 nC, representing increases of 10% and 18%, respectively.

Using PBS and copper films as triboelectric materials, the fabricated TENG can convert a pulsed alternating current into direct current through a simple rectifier circuit. Fig. 6(a) shows the charging of capacitors using a triboelectric nanogenerator through a full-bridge rectifier circuit. This setup charges commercial capacitors, providing a stable and continuous power supply for small electronic devices. Under a contact load of 30 N, a separation distance of 15 mm, and a frequency of 2 Hz, capacitors of 1  $\mu\text{F}$ , 4.7  $\mu\text{F}$ , and 10  $\mu\text{F}$  are charged to 1.5 V in 24 s, 60 s, and 125 s, respectively. The TENG (25  $\times$  25 mm²) is constructed as shown in the device structure in Fig. 6(b). The TENG, connected through a full-bridge rectifier circuit, can light up 43 commercial LED lights, as shown in Fig. 6(c).

## Conclusions

Flexible PBS exhibits shape adaptability and adhesiveness, allowing it to adhere well to the human body. Due to its internal cross-linking structure, it possesses self-healing properties, achieving a self-healing efficiency of 93.2% within 3 minutes at room temperature. As the boric acid content in PBS increases, the electrical output performance of the films improves. When the boric acid content reaches 33 wt%, the  $V_{\rm oc}$  and  $Q_{\rm sc}$  increase by 15% and 20%, respectively, compared to a boric acid content of 8 wt%. However, the mechanical properties decrease with higher boric acid content. The output decreases with increasing loading frequency: cosine loading mode yields higher output, and the output increases with longer loading times.

#### Author contributions

J. H. Liang: conceptualization, formal analysis, investigation, methodology, validation, visualization, and writing original draft. R. Zhao: supervision, investigation, review and editing. J. L. Li and D. Zhao: conceptualization, investigation, and methodology. P. L. Liu: investigation and writing original draft. C. Y. Tian: funding acquisition, supervision, review and editing. N. Sun: conceptualization, funding acquisition, supervision, review and editing.

# Data availability

The data supporting this article have been included as part of the manuscript. Additional data related to this study may be requested from the corresponding author.

#### Conflicts of interest

The authors have no conflicts to disclose.

## Acknowledgements

This work was financially supported by the National Natural Science Foundation of China (Grant No. 51105223) and the Tribology Science Fund of the State Key Laboratory of Tribology (No. SKLTKF15A02).

#### References

- 1 J. Henniker, Triboelectricity in Polymers, *Nature*, 1962, **196**(4853), 474–474.
- 2 Z. L. Wang and W. Z. Wu, Nanotechnology-enabled energy harvesting for self-powered micro-/nanosystems, *Angew. Chem., Int. Ed.*, 2013, **51**(47), 11700–11721.
- 3 H. Guo, J. Wan, H. X. Wu, *et al.*, Self-Powered multifunctional electronic skin for a smart anti-counterfeiting signature system, *ACS Appl. Mater. Interfaces*, 2020, **12**(19), 22357–22364.
- 4 Y. Zi, H. Guo, Z. Wen, *et al.*, Harvesting low-frequency (<5 Hz) irregular mechanical energy: A possible killer application of triboelectric nanogenerator, *ACS Nano*, 2016, **10**(4), 4797–4805.
- 5 X. L. Chen, W. Tang, Y. Song, *et al.*, Power management and effective energy storage of pulsed output from triboelectric nanogenerator, *Nano Energy*, 2019, **61**, 517–532.
- 6 B. Yang, W. Zeng, Z. H. Peng, et al., A fully verified theoretical analysis of contact-mode triboelectric nanogenerators as a wearable power source, Adv. Energy Mater., 2016, 6(16), 1600505.
- 7 W. Kim, H. J. Hwang, D. Bhatia, et al., Kinematic design for high performance triboelectric nanogenerators with enhanced working frequency, Nano Energy, 2016, 21, 19–25.
- 8 T. Cheng, Y. Li, Y.-C. Wang, *et al.*, Triboelectric nanogenerator by integrating a cam and a movable frame for ambient mechanical energy harvesting, *Nano Energy*, 2019, **60**, 137–143.
- 9 K. W. Han, J. N. Kim, A. Rajabi-Abhari, *et al.*, Long-lasting and steady triboelectric energy harvesting from low-frequency irregular motions using escapement mechanism, *Adv. Energy Mater.*, 2021, 11(4), 2170015.
- 10 S. Nuthalapati, A. Chakraborthy, I. Arief, et al., Wearable high-performance MWCNTs/PDMS nanocomposite-based triboelectric nanogenerators for haptic applications, *IEEE J. Flexible Electron.*, 2024, 3(9), 393–400.
- 11 S. Hajra, S. Panda, H. Khanberh, *et al.*, Revolutionizing Self-Powered Robotic Systems with Triboelectric Nanogenerators, *Nano Energy*, 2023, **115**, 108729.
- 12 M. Tang, P. Zheng, K. Wang, *et al.*, Autonomous self-healing, self-adhesive, highly conductive composites based on a silver-filled polyborosiloxane/polydimethylsiloxane

- double-network elastomer, *J. Mater. Chem. A*, 2019, 7(48), 27278–27288.
- 13 S. Potu, A. Kulandaivel, B. Gollapelli, *et al.*, Oxide-based triboelectric nanogenerators: Recent advances and future prospects in energy harvesting, *Mater. Sci. Eng.*, *R*, 2024, **161**, 100866.
- 14 S. Potu, M. Navaneeth, R. K. Rajaboina, et al., High-per-formance and low-cost overhead projector sheet-based triboelectric nanogenerator for self-powered cholesteric liquid crystal, electroluminescence, and portable electronic devices, ACS Appl. Energy Mater., 2022, 5(11), 13702–13713.
- 15 G. M. Rani, S. M. Ghoreishian, R. Umapathi, et al., A bio-compatible triboelectric nanogenerator-based edible electronic skin for morse code transmitters and smart health-care applications, Nano Energy, 2024, 128, 109899.
- 16 J. Sun, X. Pu, M. Liu, et al., Self-healable, stretchable, transparent triboelectric nanogenerators as soft power sources, ACS Nano, 2018, 12(6), 6147–6155.
- 17 J. Deng, X. Kuang, R. Liu, et al., Vitrimer elastomer-based jigsaw puzzle-like healable triboelectric nanogenerator for self-powered wearable electronics, Adv. Mater., 2018, 30(14), e1705918.
- 18 M. Tang, W. T. Wang, D. H. Xu, et al., Synthesis of structure-controlled polyborosiloxanes and investigation on their viscoelastic response to molecular mass of polydimethylsiloxane triggered by both chemical and physical interactions, *Ind. Eng. Chem. Res.*, 2016, 55(49), 12582–12589.
- 19 C. Y. Liu, Study of mechanical properties of high temperature vulcanized silicone rubber modified by polyborosiloxane, Xi'an Univ. Technol. (XUT), Xi'an, 2020.
- 20 S. Y. Feng, J. Zhang and M. J. Li, *Silicone polymers and their applications*, Chem. Ind. Press, Beijing, 2004.
- 21 X. F. Li, D. A. Zhang, K. W. Xiang, *et al.*, Synthesis of polyborosiloxane and its reversible physical crosslinks, *RSC Adv.*, 2014, 4(62), 32894–32901.
- 22 E. D'elia, S. Barg, N. Ni, *et al.*, Self-healing graphene-based composites with sensing capabilities, *Adv. Mater.*, 2015, 27(32), 4788–4794.
- 23 Y. H. Chen, X. Pu, M. M. Liu, et al., Shape-adaptive, self-healable triboelectric nanogenerator with enhanced performances by soft solid-solid contact electrification, ACS Nano, 2019, 13(8), 8936–8945.
- 24 H. Ryu, J. H. Lee, T. Y. Kim, *et al.*, High-performance triboelectric nanogenerators based on solid polymer electrolytes with asymmetric pairing of ions, *Adv. Energy Mater.*, 2017, 7(17), 1700289.
- 25 Y. L. Zi, H. Y. Guo, Z. Wen, et al., Harvesting low-frequency (<5 Hz) irregular mechanical energy: a possible killer application of triboelectric nanogenerator, ACS Nano, 2016, 10(4), 4797–4805.</p>